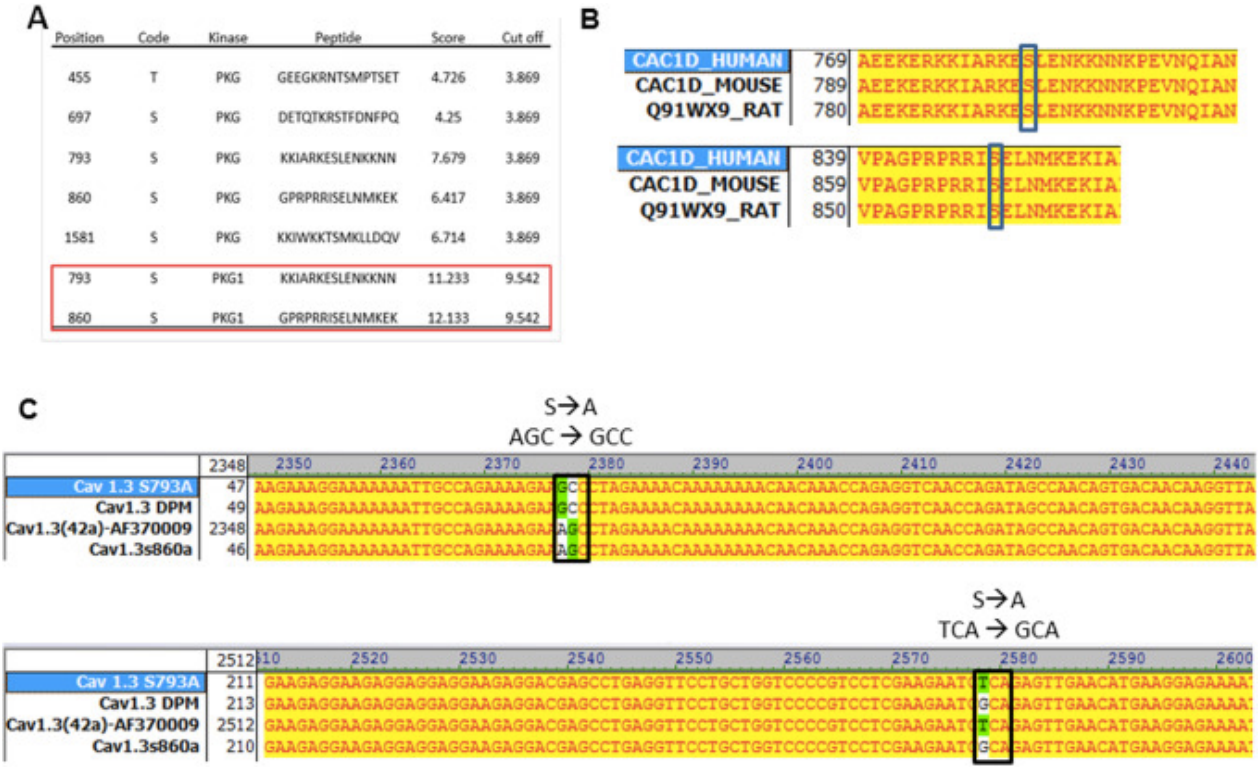


Supplemental Figure 1. A) Summary of putative phosphorylation sites localized with the GPS 2.0 (Group-based Prediction System) software. The residues with the highest score are indicated by the red box. B) Protein sequence alignment of $Ca_V1.3$ channel sequences in different species as indicated. The blue boxes indicate conserved serine residues. C) Sequence analysis of RT-PCR amplification products from rat RNA. The black boxes indicate the codon triplets with the Ser to Arg amino acid changes at positions 793 and 860.

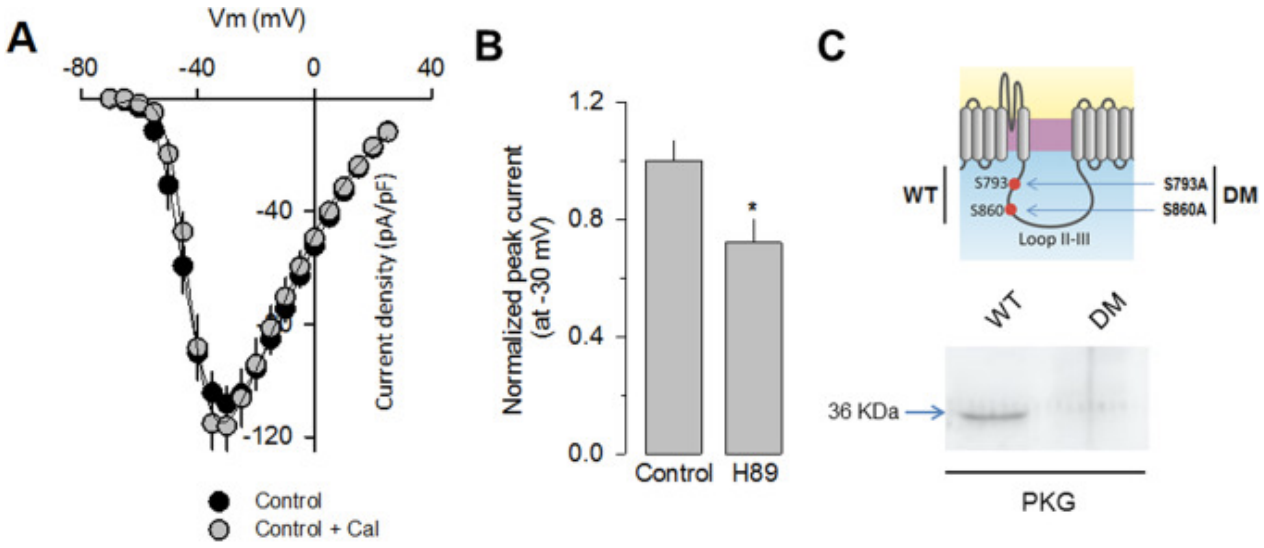


Supplemental Figure 2. A) Application of the phosphatase inhibitor Calyculin A does not modify current density through recombinant L-type $Ca_V1.3$ channels. Average current density-voltage relationships for $I_{Ba}$ recorded from HEK-293 cells expressing $Ca_V1.3/Ca_V\alpha_2\delta\text{-}1/Ca_V\beta_3$ channels in the absence and presence of Calyculin (10 nM). B) Application of the PKA blocker H-89 inhibits current density through recombinant L-type $Ca_V1.3$ channels harboring the S793A mutation. Average peak current density recorded from HEK-293 cells expressing wild-type and mutant $Ca_V1.3$ channels in the absence and presence of H-89 (100 nM). C) Purified recombinant $Ca_V1.3$ wild-type and double phosphorylation mutant (DPM) constructs (amino acid residues 2154 to 2254) were subjected to phosphorylation by PKG *in vitro* (left panel). The upper panel shows the position the potential sites of PKG phosphorylation, where the point mutations were introduced.

Suppl Table 1

| Gene | Sequence | Size (bp) |
|---|---|---|
| PKG | AAGATTCTCATGCTCAAGGA<br>CAGCTCCAAGTTCTTCATGA | 300 |
| actin | AAGATGACCCAGATCATGTT<br>GAGTACTTGCGCTCAGGAGG | 662 |

Suppl Table 2

| Protein Description | Gene | Taqman® assay |
|---|---|---|
| actin, beta | *Actb* | Rn00667869_m1 |
| calcium channel, voltage-dependent, N type, alpha 1B subunit | *Cacna1b* | Rn00595911_m1 |
| calcium channel, voltage-dependent, L type, alpha 1C subunit | *Cacna1c* | Rn00709287_m1 |
| calcium channel, voltage-dependent, beta 2 subunit | *Cacnb2* | Rn00587789_m1 |
| calcium channel, voltage-dependent, beta 3 subunit | *Cacnb3* | Rn00432233_m1 |

Supplemental Table 1. Nucleotide sequence of the oligonucleotides used in this study.

Suppl Table 3

| | Control | Control 8Br | S793A | S793A 8Br | S860A | S860A 8Br | DPM | DPM 8Br |
|---|---|---|---|---|---|---|---|---|
| Gmax | 1.3522 | 0.8548 | 1.6227 | 0.922 | 1.4162 | 1.6466 | 1.3086 | 1.3862 |
| k | 4.0246 | 3.4037 | 3.0069 | 3.5248 | 3.2294 | 3.8236 | 3.0381 | 3.6321 |
| V½ | -45.2504 | -41.2092 | -46.7998 | -49.0069 | -42.7281 | -42.8331 | -46.5765 | -47.2449 |

Supplemental Table 2. TaqMan-based Real-Time PCR assays for estimation of the number of copies of the $Ca_V\alpha_1$ pore-forming and the $Ca_V\beta$ auxiliary subunits.

Supplemental Table 3. Comparison of parameters derived from Boltzmann fits to *I-V* curves for WT and $Ca_V1.3$ channel mutants.